

Microstructure and Mechanical Properties of Magnesium ZRE1 (Mg-Zn-Zr) Alloy with Rare Earth Element (Samarium) Addition

Ikhwan Shah Tisadi Tukiati¹, Nur Kamilah Yusuf^{1*}, Haikal Khaireez¹, Sami Al-Alimi^{1**}, Mohd Amri Lajis¹, Shazarel Shamsudin¹, Nasha Emieza Ruhaizat¹

¹*Sustainable Manufacturing and Recycling Technology (SMART), Advanced Manufacturing & Materials Center (AMMC), Faculty of Mechanical and Manufacturing Engineering, Universiti Tun Hussein Onn Malaysia, 86400 Johor, Malaysia*

Abstract. The influences of rare earth (RE) samarium (Sm) added contents to ZRE1 (Mg-Zn-Zr) magnesium (Mg) cast alloy over strength properties to be investigated. Sm at 0.5, 1.0, 1.5, and 2.0 wt.% were added separately as an alloying element to ZRE1 alloy. Optical Microscope (OM), X-ray powder diffraction (XRD), and scanning electron microscope Energy-dispersive X-ray (SEM/EDS) were used to investigate the microstructure of alloy, while mechanical properties investigated include Ultimate Tensile Strength (UTS) and Micro-Hardness (MH) tests. The result revealed that as the Sm level reached 1.5 wt.%, the grain size decreased by 20.9 %. Additionally, UTS and Yield Strength (YS) showed improvements of 8.5 % and 7.9 %, respectively, with the addition of 1.5 wt.% of Sm. In addition, elongation and hardness have been improved by 32.3 % and 10.9 % respectively at 1.5 wt.% Sm addition. Mg-Zn-Ce-Sm was formed as a new phase upon the addition of Sm and was detected via XRD analysis. The addition of Sm to the ZRE1 alloy had significant effects on the refinement of the material's microstructure, leading to an increase in its mechanical and physical properties. Therefore, the new ZRE1-RE magnesium alloy was developed.

Keywords: Magnesium ZRE1 alloy; Metal forming and materials refinement; Microstructure and mechanical properties

1. Introduction

Magnesium (Mg) alloys have great potential as engineering materials because of their high specific strength, low density, high stiffness, excellent electromagnetic shielding characteristics, superior damping capacity, and good machinability (Kristanto, Gusniani, and Ratna, 2015; Rzychoń, Kiełbus, and Szala, 2008). Mg alloys have sparked enormous interest in aerospace, defense, electronics, and automotive industries in recent years. However, Mg application in engineering is still limited due to high material cost, poor corrosion resistance as well as low strength, durability, fatigue life, ductility, toughness, and creep resistance (Purnama *et al.*, 2020; Kiani *et al.*, 2017; Adrian, 2012). The addition of RE metal to Mg alloy could overcome its weakness and further improve its properties.

According to (Jahedi, McWilliams, and Knezevic, 2018), the rare-earth elements containing Mg alloys could (i) increase ductility and strength while reducing the anisotropy

*Corresponding author's email: nurkamilah@uthm.edu.my, Tel.: 6074537325; Fax: 6074536080

**Corresponding author's email: samiabdo@uthm.edu.my, Tel.: 6074537706; Fax: 6074536080

doi: [10.14716/ijtech.v15i1.6057](https://doi.org/10.14716/ijtech.v15i1.6057)

and tension/compression asymmetry, (ii) higher resistance to creep and corrosion, (iii) improve biodegradability, (iv) reduce flammability, (v) retain high-temperature strength, (vi) improve elongation to fracture, (vii) grain boundary strengthening and (viii) improve fatigue resistance and fracture toughness. Zinc (Zn) is the second most effective and common alloying material to produce Mg alloy after aluminum (Al). The addition of zinc in Mg alloy increases room-temperature strength, increases alloy fluidity in casting, and improves corrosion resistance (Moosbrugger, 2017). In addition, recent research shows that adding RE elements to Mg-Zn alloy can further improve various mechanical and chemical properties. The most common RE metal additions in Mg-Zn alloy are Cerium, Lanthanum, Gadolinium, Neodymium, and Yttrium (Al-Alimi *et al.*, 2021; Materialstechnology, 2019).

ZRE1 is one of many Mg alloys available in the market nowadays. ZRE1 is an Mg alloy containing RE metal with the addition of zinc and zirconium, forming Mg-RE-Zn-Zr (Ahmad *et al.*, 2017a). The detailed chemical composition of the ZRE1 alloy is shown in Table 1. ZRE1 exhibits superior high-temperature creep resistance (Ferro, Saccone, and Delfino, 2013) and resistance to stress relaxation compared to that of benchmark alloy AE42 (Rzychoń, Kiełbus, and Szala, 2008). The presence of RE in ZRE1 makes the alloy free of microporosity and holds up to hot cracking, which at the same time offers good weldability (Ferro, Saccone, and Delfino, 2013). Currently, ZRE1 is used in the aerospace industry for intermediate casings on Tay engines, gearboxes of RB211 engines, and gearboxes of Tay engines (Materialstechnology, 2019).

Table 1 Chemical composition of the ZRE1 alloy in wt.% (Rzychoń, Kiełbus, and Szala, 2008)

Zn	RE	Zr	Ni	Si	Cu	Mn	Fe	Mg
2.7	3.18	0.53	<0.001	<0.01	<0.01	0.02	0.002	balance

Research by (Ahmad *et al.*, 2017a) explored the effect of Praseodymium (Pr) addition on the microstructure and hardness of cast ZRE1 Mg alloy. They reported that 1 wt.% Pr addition on ZRE1 cast alloy reduces the grain size of ZRE1 alloy by around 37%. Meanwhile, the addition of Pr improves the hardness value of ZRE1 by 24 %. This is due to the effect of grain refinement and the effect of the second phase (Mg-Zn)₁₂ RE and intermetallic compound (Mg-Zn-Ce-Pr). In their study, Ahmad *et al.* (2016) extended their research to examine the effects of Gadolinium on the microstructure and hardness of ZRE1 cast alloy. They found out that the addition of 3 wt.% heavy RE Gadolinium (Gd) reduce grain size by 28% and increased the volume fraction of eutectic secondary phase while at the same time improving the hardness by 34%.

Samarium (Sm) is one of the RE elements with huge potential to form Mg alloy. Researchers have been applied Sm as an alloying element for various Mg alloys for a long time (Guan *et al.*, 2018). The addition of Sm to Mg alloy could reduce grain size, improve corrosion resistance, enhance yield strength and ultimate tensile strength, improve toughness, and at the same time, better elongation to Mg alloys, as shown in Table 2. However, to the best of our knowledge, researchers still have not given any attention to the influence of Sm addition on microstructures and mechanical properties of as-cast ZRE1 alloy. Sm is an orthorhombic structure with good solid-solution and precipitation strengthening in Mg alloys (Li, Xu, and Tong, 2019). Additionally, Sm costs are lower compared to Nd, Y, and Gd in the market (Lucas *et al.*, 2014). Based on the Rare Earth Metal price, Sm is the cheapest RE of all, only beaten by Ce and La in price (Institute of Rare Earths and Strategic Metals eV, 2020). Additionally, Sm is the seventh most abundant RE in earth's

crust, with 7.1 ppm. Among all earth's elements, Sm is the 40th most abundant and widely available than silver, tin, and gold (Enghag, 2004).

Hence, researchers have conducted studies on the effect of Sm addition to various magnesium systems such as Mg-6.0Zn-0.5Zr alloy (ZK60) (Guan *et al.*, 2018), Mg-11Gd-2Y-0.6Al (Chen *et al.*, 2019), Mg-Al-Zn (AZ61) (Anawati, Asoh, and Ono, 2018; Chen *et al.*, 2015) Al-Zr-Ce (Kirman, Zulfia, and Suharno, 2016) and Mg-5Y-2Nd-0.5Zr (Yunwei *et al.*, 2018). It is found the application of 1.5 wt.% Sm additive in Mg- 6.0Zn-0.5Zr alloy (ZK60) refined the grains of the as-cast sample, while the extruded sample shows even finer (Guan *et al.*, 2018). At the same time, Sm addition further improves the strength of ZK60 alloy due to fine grain strengthening and precipitation strengthening. This outcome is consistent with Chen *et al.* (2019) findings, where they demonstrated a refined grain structure and improved tensile strength in the microstructure and mechanical properties of the Mg-Gd-Y-Sm-Al alloy. This corresponds to a study on the effects of samarium addition to the AZ61 (Mg-Al-Zn) magnesium alloy, resulting not only in a refined microstructure but also in improved ultimate tensile strength and elongation. However, excessive Sm addition could cause the coarsening of grain, leading to the decline of strength and plasticity (Rady *et al.*, 2019; Al-Alimi, Lajis, and Shamsudin, 2017).

Table 2 Previous study on RE addition to Mg alloy

Researcher	Mg alloy	RE addition	Result
Liu <i>et al.</i> (2016)	Mg-Zn-Zr	Ce, Y	Improve YS, UTS
Rogal <i>et al.</i> (2019)	E21 Mg-Gd-Nd-Zn-Zr	Nd-Y	Improve YS, plasticity, hardness
Ahmad <i>et al.</i> (2017a)	ZRE1 Mg-RE-Zn-Zr	Pr	Reduces grain size, improves hardness
Ahmad <i>et al.</i> (2016)	ZRE1 Mg-RE-Zn-Zr	Gd	Increased volume fraction, improved hardness
Guan <i>et al.</i> (2018)	ZK60 Mg-Zn-Zr	Sm	Improves strength
Chen <i>et al.</i> (2019)	Mg-Gd-Y-Sm-Al	Sm	Improved TS, microstructure
Chen <i>et al.</i> (2015)	AZ61 Mg-Al-Zn-Mn	Sm	Refined microstructure, improved UTS, EL
Yunwei <i>et al.</i> (2018)	Mg-Y-Nd-Zr	Sm	Improve UTS, YS and hardness
Liu <i>et al.</i> (2021)	AZ41 Mg-Al-Zn-Mn	Sm	Improve UTS, YS and EL
Rokhlin <i>et al.</i> (2021)	Mg-Gd	Sm	Increase strength

Samarium also has unique properties that make it useful for various applications other than as an alloying element in metals. Chauhan, Lohra, and Langyan (2020) found that ternary samarium (III) complexes exhibit fascinating optical properties, making them potentially useful in bio-assays, electroluminescent devices, and liquid lasers. Luo *et al.* (2019) synthesized a novel samarium complex that emits red light and has potential as a red light emitting material for LEDs. Meanwhile Hashmi *et al.* (2019) studied the effects of samarium incorporation in ZnO thin films and found that it affected the optical and electrical characteristics of the films, making them suitable for use in optical devices for UV and blue emission. Marzouk and Hammad (2020) found that samarium oxide affects the structural and optical properties of bismuth glass, making it suitable for photonic applications. Sadeq and Morshidy (2020) showed that samarium oxide influences the structural, optical, and electrical properties of alumino-borate glasses, making them good optical filters. Overall, the papers suggest that samarium has unique properties that make it useful for various applications in optics, electronics, and materials science.

2. Methods

An Mg base alloy (ZRE1 Mg cast) was supplied by ILM Ventures Ltd., Kuala Lumpur,

Malaysia in ingot cast. The base alloy was melted in an electrical resistance furnace with a steel crucible under a cover-gas mixture of 99 vol% Argon (Ar) and 1 vol% of Sulfur hexafluoride (SF₆), both from Linde and supplied by Linde Malaysia Sdn Bhd, Kuala Lumpur, Malaysia. Sm from Merck, Kuala Lumpur, Malaysia was added in contents of 0.5 wt.%, 1.0 wt.%, 1.5 wt.% and 2.0 wt.% separately as small pieces after the base alloy melted at approximately 730°C. After the addition, the melt was stirred for approximately 30 minutes to ensure stabilization, homogeneous composition, and dissolution of the alloying elements. The molten metal was then poured into a permanent steel mold preheated to 400°C. The cast was then left to cool down to room temperature before being removed from the mold. The graphical abstract of the research methodology and the melt-stir casting setup are shown in Figure 1 and Figure 2, respectively.

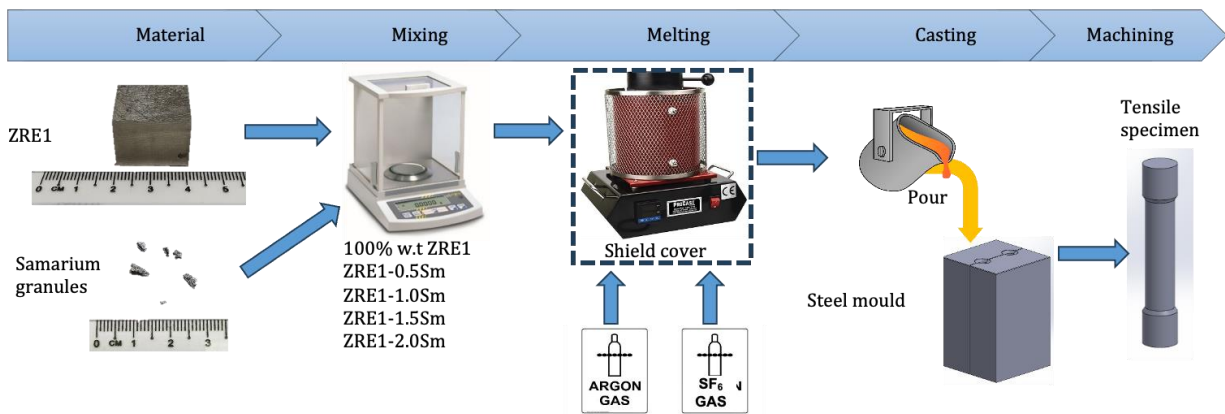


Figure 1 Graphical Abstract of Research Methodology

All microstructure analysis samples were cut from the center of the cast alloy. The sample was then prepared using the ASTM Standard Guide for Preparation of Metallographic Specimens (ASTM, 2011; Geels *et al.*, 2007) grinding/polishing procedures before final etching with 4 vol% picric acid in ethanol solution. An optical microscope (Nikon Eclipse LV150NL) and image analysis software (IMT i-Solution DT v12.0) was used to measure the grain size and volume fraction. In addition, the specimens were examined using a scanning electron microscope (SEM) equipped with an energy-dispersive X-ray spectrometer (EDS) (Hitachi SU1510) and X-ray powder diffraction (XRD) (Bruker D8 Advance) for microstructure study and phase formed in the Mg alloy. A permanent preheated mild-steel mold was used to produce cylindrical tensile test specimens. The melt was neatly poured at 730 ± 5 °C into the preheated permanent steel mold after being skimmed and stirred. The castings were machined using CNC turning to achieve precise specimen dimensions based on the requirement of ASTM B557M (ASTM International, 2015).

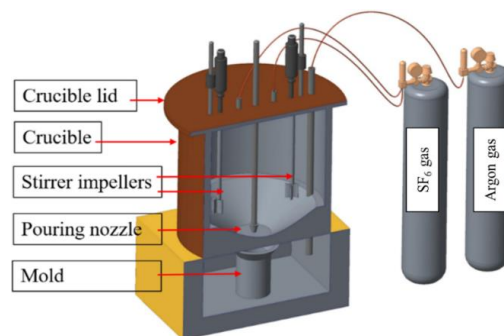


Figure 2 Melt-stir casting setup with Argon and SF₆ gas shield

3. Results and Discussion

XRD analysis was performed on Figure 3 and the selected specimens to identify the phases present in the ZRE1-xSm alloys; the results are shown in 1. It can be seen that the base alloy consisted of α -Mg phase and Mg-Zn-Ce secondary intermetallic phase. The α -Mg phase was found in a hexagonal structure, while the secondary phase was a tetragonal structure. The position of peaks originating from Mg are exactly equivalent to Mg standard peaks as reported by (Sheggaf *et al.*, 2017; Wang *et al.*, 2014). α -Mg phase was found to possess a hexagonal structure with crystallographic parameters of ($a = 3.20936$; $b = 3.20936$; $c = 5.21120$) Å while the Mg-Zn-Ce phase was tetragonal with ($a = 3.83100$; $b = 3.83100$; $c = 3.83100$) Å crystallographic parameters. Similar phases were obtained by other Mg-Zn-Zr with RE addition alloys (Sheggaf *et al.*, 2017; Liu *et al.*, 2016).

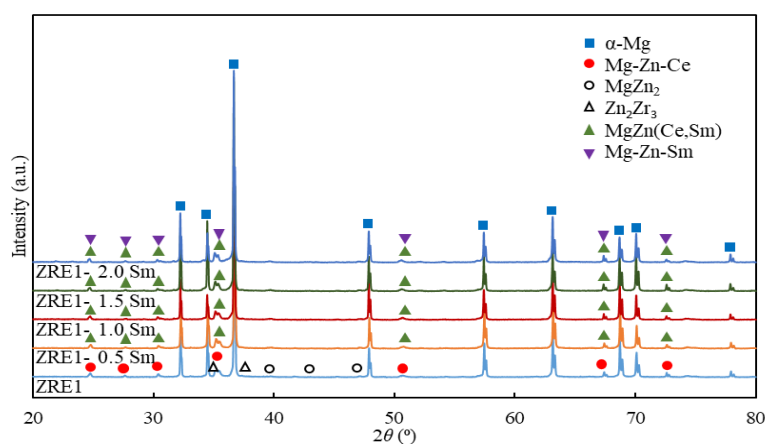


Figure 3 XRD pattern of ZRE1-xSM alloys

Furthermore, the XRD pattern also detected other phases in the base ZRE1 alloy, which is MgZn_2 and Zn_2Zr_3 . These phases form in small amounts and dissolve inside the Mg matrix of the base alloy (Sheggaf *et al.*, 2017; Liu *et al.*, 2016). MgZn_2 has a hexagonal crystal structure with crystallographic parameters ($a = 5.22250$; $b = 5.22250$; $c = 8.56840$) Å while Zn_2Zr_3 has a tetragonal crystal structure and ($a = 7.63300$; $b = 7.63300$; $c = 6.96500$) Å crystallographic parameters. The addition of the rare earth element Sm to the ZRE1 base alloy resulted in the detection of the $\text{MgZn}(\text{Ce},\text{Sm})$ phase within the sensitivity limits of XRD, manifesting at the same peaks as the secondary phase of the ZRE1 base alloy. The emergence of this $\text{MgZn}(\text{Ce},\text{Sm})$ phase indicates the transformation of a new phase from the secondary phase of the ZRE1 base alloy (Sheggaf *et al.*, 2017). The new $\text{MgZn}(\text{Ce},\text{Sm})$ intermetallic phase has a hexagonal crystal structure with ($a = 14.61900$; $b = 14.61900$; $c = 8.70800$) Å crystallographic parameters. Additionally, the Mg-Zn-Sm intermetallic phase was detected at ZRE1-2.0 Sm alloy at the same peak of $\text{MgZn}(\text{Ce},\text{Sm})$. This phase shows that both phases were crystallized and combined at the alloy grain boundaries (Sheggaf *et al.*, 2017; Liu *et al.*, 2016). Previous studies also found the same result, where the MgZnRE phase was formed as a secondary intermetallic phase (Sheggaf *et al.*, 2017).

The addition of Sm does not change the crystalline size and shape of α -Mg before and after adding Sm. Both samples have a hexagonal structure with crystallographic parameters of ($a = 3.20936$; $b = 3.20936$; $c = 5.21120$) Å and structure angle alpha 90° - beta 90° - gamma 120° . However, there are slight changes in the crystalline size of the MgZn_2 crystal structure. Even though both samples possess MgZn_2 in a hexagonal structure, the size decreases from ($a = 5.22250$; $b = 5.22250$; $c = 8.56840$) Å for base ZRE1 alloy to ($a = 5.22100$; $b = 5.22100$; $c = 8.56700$) Å. Small changes in the c value may be due to the addition of Sm, which has a large-sized atom in comparison to a small atom of Mg, pushing

the $MgZn_2$ crystal compound to squeeze slightly and squish its hexagonal structure size. According to one theory by [Ke-Jie *et al.* \(2009\)](#), when a solid solidifies, Sm atoms are squeezed through the solid-liquid barrier, causing constitutional supercooling and assisting in the development of a nucleus.

Furthermore, the mechanical properties of the material are mainly caused by the type, distribution, amount, and morphology of the intermetallic phase ([Shenggaf *et al.*, 2017](#)). The $MgZnRE$ intermetallic phase has a long periodic piling ordered structure and is coherent with the α -Mg phase matrix. In Figure 4, the property-making $MgZnRE$ phase becomes a strengthening mechanism of MgZn alloys, thus improving mechanical properties ([Liu *et al.*, 2016](#)). The strengthening of Mg alloys is due to the solid solution of the RE atoms in borderline sizes together with secondary phase hardening of the $MgZnRE$ intermetallic compound ([Yang *et al.*, 2008](#)). The RE addition to Mg-Zn alloys formed intermetallic phases that improved the strength of the Mg alloy. This improvement was caused by grain boundary strengthening of the $MgZnRE$ phase and $MgZn(Ce, Sm)$ phase crystallized along the grain boundaries. At the same time, the matrix phase and intermetallic phase form a rigid atomic bonding by obstructing slip dislocation of MG-Zn-RE alloy planes, thus strengthening the material further ([Tekumalla *et al.*, 2014](#)). Furthermore, both secondary phases, $MgZn_2$ and Zn_2Zr_3 from ZRE1 base alloy, disappear completely with the addition of Sm. This may be due to the addition of RE, which reduces the solubility of Zn in the Mg matrix. As a result, the phases may not develop or may form in small quantities, potentially beyond the detection limit of the XRD spectrum ([Huang *et al.*, 2009](#)).

Figure 4 shows optical microscopes taken from the ZRE1 base alloy and alloy with Sm addition. The alloy microstructure consists of α -Mg matrix (marked A) and secondary phase crystalline along the grain boundary (marked B). The secondary intermetallic phase forms in location B are known from XRD data as Mg-Zn-Ce, $MgZn_2$, and Zn_2Zr_3 . The secondary phase at the microstructure grain boundary shows massive morphology in a dark contrast color. The Sm addition to the alloy changes the microstructure of the ZRE1 base alloy. Similarly, research by ([Shenggaf *et al.*, 2017](#)) and ([Kusrini *et al.*, 2021](#)) showed that ZRE1 base alloys microstructure changes with the addition of Pr.

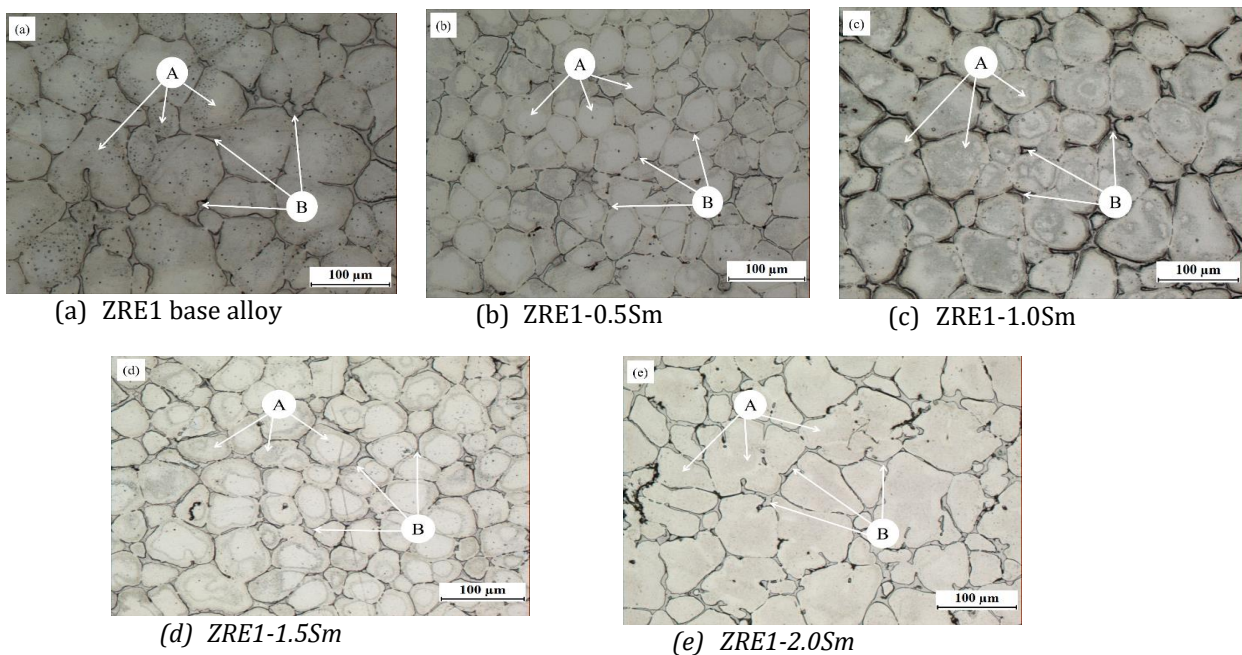


Figure 4 Microstructure image (a) ZRE1 base alloy and (b-e) ZRE1 with Sm addition using optical microscope

The addition of Sm shows a significant effect on ZRE1 grain size in Figure 5, where the addition of 0.5 wt.% Sm reduces the grain size significantly by about 13% due to an increase in the coherency time of the alloy (Ahmad *et al.*, 2017b). Previous study shows that the dendrite impingement rate occurs at a low pace while occurs at a higher speed for small grain sizes (StJohn *et al.*, 2005). The increase of Sm content shows a reduction in the grain size of the alloy, which obtains 33.33 μm grain size of 0.5 wt.%, 31.53 μm for 1.0 wt.%, 30.43 μm for 1.5 wt.% and 32.41 μm for 2.0 wt.% Sm. The trend is parallel to the outcome of another similar Mg-RE research. It also has been reported by (Guan *et al.*, 2018) that the addition of Sm is effective for grain refinement of ZK60 alloy (Mg-6.0Zn-0.5Zr) due to the secondary phase containing Sm that restricts grain growth. The mechanism behind the grain refinement effect of rare earth on magnesium alloy is that RE acts as nucleation sites for recrystallization and grain refinement (Ding-qian, 2008). Additionally, the formation of high melting-point Mg-RE phases can act as the heterogeneous nucleation cores of the α -Mg matrix and refine the grain size (Zhang, Wang, and Li, 2017).

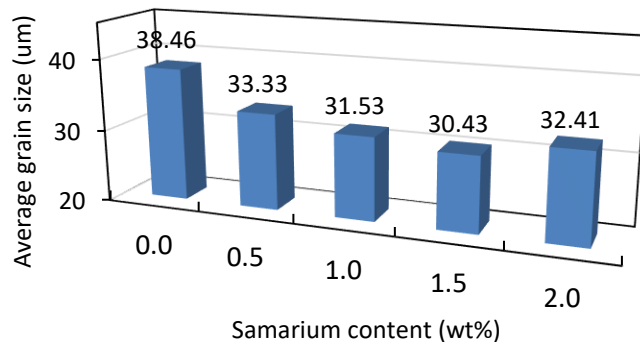


Figure 5 Effect of Sm addition on the average grain size of ZRE1 magnesium alloy

The effect of Sm addition on the volume fraction of ZRE1 alloy has been shown in Figure 6, where the addition of Sm shows a significant effect on ZRE1 volume fraction. The addition of Sm increased the volume fraction of Mg alloy from 14.30 % for the base alloy to 17.64 % for 0.5 wt. % Sm addition, 19.28 % for 1.0 wt. % Sm, 20.59 % for 1.5 wt. % Sm and 22.77 % for 2.0 wt. % Sm addition. The trend is parallel to the outcome of other similar Mg-RE research (Ahmad *et al.*, 2017b; Wang *et al.*, 2014). The study conducted by Ryou *et al.* (2018) examines the correlation between grain size and grain boundary volume fraction. The findings of the investigation indicate that a reduction in grain size leads to an increase in the proportion of grain boundaries, owing to alterations in the structure, including a rise in the volume fraction of triple junctions.

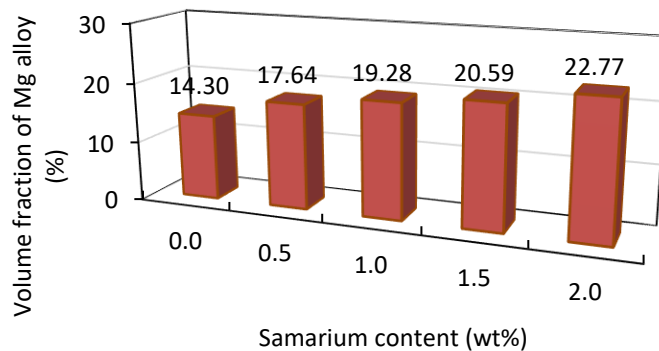


Figure 6 Effect of Sm addition on the volume fraction of ZRE1 magnesium alloy

Figure 6 shows the volume fraction of the intermetallic compounds growing as a result of the addition of Sm to the ZRE1 alloy. At the same time, the continuous networks of eutectic compounds surround the primary α -Mg grains where have a tendency to become separated from the grains when it's refined (Sheggaf *et al.*, 2017). Furthermore, the grain boundary width becomes thicker as the content of Sm increases because Sm has a tendency to combine with the secondary phases. It is supported by the research of (Guan *et al.*, 2018) that the addition of Sm increases the volume fraction of secondary intermetallic phases of ZK60 alloy.

Figure 7 (a) shows SEM micrograph and EDS microanalyses of ZRE1 base alloy and ZRE1 alloy with 2.0 wt.% Sm addition shown in (b). SEM observations for base alloy microstructure in (a-i) consist of α -Mg grains, marked A, while surrounded by a secondary phase crystallized along the grain boundaries like a vast morphology marked B. The EDS spectrum of base alloy shown in (a-ii) is indicated by points consistently showing the composition of the α -Mg matrix at region marked A and the secondary phase of the base alloy at region B. The base alloy matrix phase comprises magnesium, zinc, and a small amount of zirconium, while the secondary intermetallic phase contains magnesium, zinc, and cerium.

SEM image of ZRE1 with 2.0 wt.% Sm alloy shown in (b-i) exposed a composition of the α -Mg matrix at region marked A, and two types of intermetallic phases (marked B and C) crystallized along the grain boundaries. The EDS result in (b-ii) shows that the intermetallic phase at point B was Mg-Zn-Ce-Sm while Mg-Zn-Sm formed at point C. The addition of more than 2.0 wt.% Sm to base alloy shows new Mg-Zn-Sm intermetallic compound formed at the grain boundary, where Sm forms its own intermetallic compound out of Mg-Zn-Ce-Sm due to lack of Ce compound to form as all intermetallic Mg-Zn-Ce-Sm (Sheggaf *et al.*, 2017). A previous study by (Li *et al.*, 2007) confirms the formation of the Mg-Zn-RE phase, where two types of RE combined with Mg and Zn to form the Mg-Zn-RE phase. Their research adding Nd and Y into Mg-Zn-Zr base alloy and forming Mg-Zn-Nd-Y-Zr alloys improved the ultimate strength and elongation, as shown in Figure 8. The Mg-Zn-RE phase is coherent with the α -Mg matrix phase and makes the Mg-Zn-RE compound the strengthening phase of the alloys. Incorporating rare earth elements into magnesium alloy can lead to the creation of primary phases with high melting points. These phases serve as nucleation cores for the α -Mg matrix and effectively reduce the grain size through refinement. The presence of refined grain boundaries has been observed to promote atom mobility and facilitate the emergence of secondary metallic phases situated at the grain boundary (Zhang, Wang, and Li, 2019). Region B is where the grain boundary is located, where the secondary intermetallic phase forms the Mg-Zn-Ce-Sm composition.

The effect of Sm content addition on the tensile properties of ZRE1Mg alloy is shown in Figure 8. The tensile test results include the ultimate tensile strength (UTS), yield strength (YS), and elongation (El) for the ZRE1 base alloy and the Sm-treated alloys. UTS result shows that the addition of 0.5 wt.% Sm has a small effect on the UTS of the alloy. The UTS only increased 3.2% from 150.3 MPa to 155.2 MPa compared to base alloy. However, a significant increase in UTS value for 1.0 wt.% Sm at 161.7 MPa (7.5%) and 163.2 MPa (8.5%) for 1.5 wt.% Sm. This increases due to refinement in grain size and an increase in the volume fraction of the secondary intermetallic phase (Sheggaf *et al.*, 2017; Zhang *et al.*, 2017). While at 2.0 wt.% Sm, UTS value only slightly increased to 156.2 MPa (3.9%) compared to base alloy due to there a decreasing trend in grain size value (Sheggaf *et al.*, 2017; Zhang *et al.*, 2017).

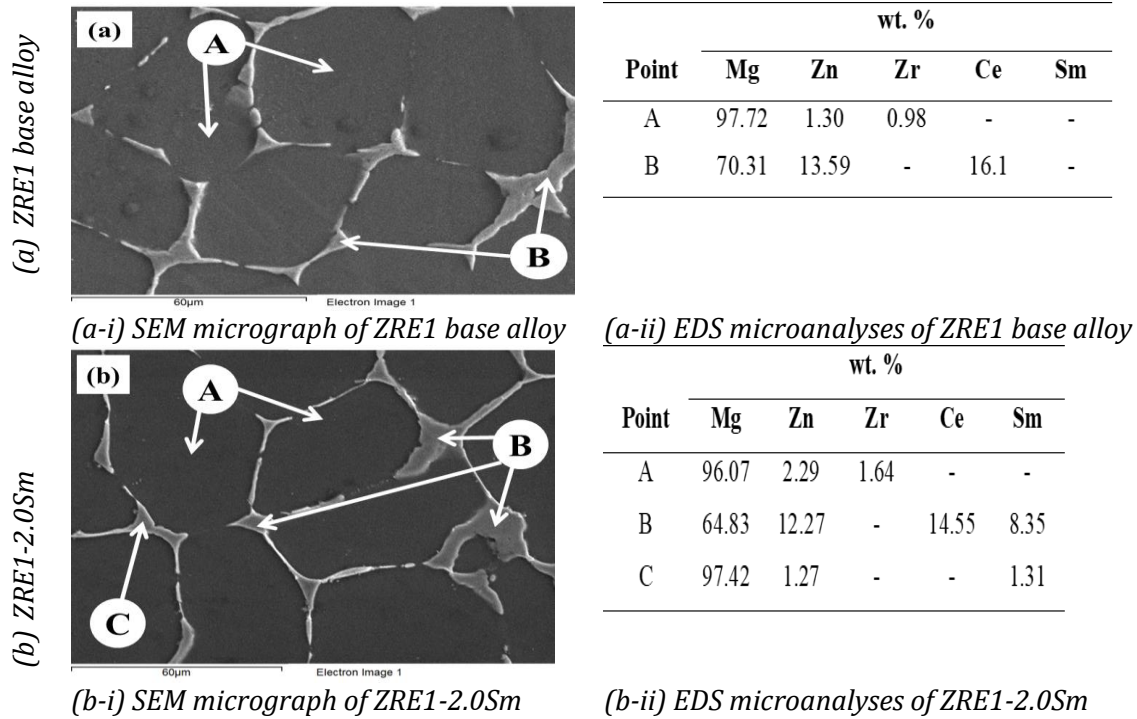


Figure 7 SEM micrograph and EDS microanalyses of (a) ZRE1 base alloy and (b) ZRE1 - 2.0 wt.% Sm

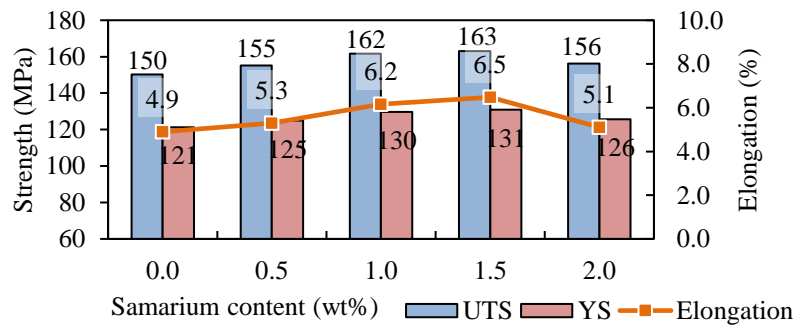


Figure 8 Effect of Sm content on the tensile properties of ZRE1Mg alloy

YS result shows that the addition of 0.5 wt.% Sm has a small effect on the YS of the alloy. The YS only increased 3.0% from 121.2 MPa to 124.9 MPa compared to base alloy. However, a significant increase in UTS value for 1.0 wt.% Sm at 129.7 MPa (7.0%) and 130.9 MPa (7.9%) for 1.5 wt.% Sm. This increase is due to refinement in grain size and an increase in the volume fraction of the secondary intermetallic phase (Sheggaf et al., 2017; Zhang et al., 2017). While at 2.0 wt.% Sm, UTS value only slightly increased to 125.6 MPa (3.6%) compared to base alloy due to there a decreasing trend in grain size value (Sheggaf et al., 2017; Zhang et al., 2017). The elongation result shows that the addition of 0.5 wt.% Sm has a small effect on the elongation of the alloy. The alloy elongation only adds 8.1% from 4.9% elongation to 5.3% elongation compared to the base alloy. However, significant improvement in elongation value for 1.0 wt.% Sm at 6.2% (25.9%) and 6.5% (32.3%) for 1.5 wt.% Sm. This increase is due to refinement in grain size and an increase in the volume fraction of the secondary intermetallic phase (Zhang et al., 2017). While at 2.0 wt.% Sm, elongation value only slightly increased to 5.1% elongation (3.6%) compared to base alloy, due to there a decreasing trend in grain size value (Zhang et al., 2017).

The outcome of UTS, YS, and elongation of this study is in line with previous research by (Zhang *et al.*, 2017). They study the effects of samarium addition on the microstructure and mechanical properties of Mg-6Zn-0.4Zr magnesium alloy. They found considerable improvement in UTS and elongation by adding 2.0 wt.% Sm. However, when the content of Sm increased more, the UTS and elongation show declining possibly due to the MgZnSm phase and the morphology of eutectic phases. The finding of the current study is also consistent with those of (Li *et al.*, 2007) in the study on the effect of Nd and Y addition of as-cast Mg-Zn-Zr alloy. They found out that the addition of two types of RE (Nd and Y) improved the mechanical properties of the Mg alloy due to dendritic size refinement. However, an increase in the amount of rare earth (RE) also resulted in a rise in the quantity of interdimeric eutectic compounds. This formation deteriorates the mechanical properties of Mg alloys due to their coarseness and their location on grain boundaries. The strengthening of Mg alloys is due to a solid solution of RE atom with borderline size and also caused by secondary phase hardening (Sheggaf *et al.*, 2017).

A study by Junior *et al.* (2022) investigating the impact of copper and nickel on alloys' microhardness and modulus of elasticity revealed that the inclusion of copper resulted in a more granular microstructure, thereby promoting a decrease in the mean value of modulus of elasticity. As per the study mentioned earlier, the inclusion of copper led to the development of a rougher microstructure, which consequently reduced the mean value of the elasticity modulus. Likewise, the incorporation of samarium into the magnesium ZRE1 alloy in the present investigation is expected to elicit analogous impacts on the microstructural characteristics, thereby influencing the modulus of elasticity. The observed correlation implies that the inclusion of samarium could potentially lead to a decrease in the mean modulus of elasticity, thereby corroborating the present study's findings.

Additionally, the secondary intermetallic phase containing RE can deter the dislocation movement, therefore improving the mechanical properties. However, after the alloy achieves its peak hardness at 1.5 wt.% Sm, the hardness value trend decreased. Where the ZRE1 alloy with 2.0 wt.% Sm shows a 57.0 HV value, a reduction compared to the previous sample. This drop happens due to the increase of grain size, which starts to occur when the Sm addition reaches 1.5 wt.% Sm thus reflected a reduction trend in hardness value. Previous research by (Wang *et al.*, 2018) also shows the same hardness value trend. Their study on the effects of RE yttrium (Y) on Mg-Al-Zn alloy shows that the harness value increases with the increase in Y addition, though the trend starts moving downward after the alloy reaches its peak hardness value. This trend is due to (i) an increase of secondary intermetallic phase containing RE, leading to solid solution hardening effect, and (ii) grain size coarsening of α -Mg matrix. According to Pereira, Huang, and Langdon, (2017), smaller grain sizes were obtained, affecting microhardness and elongation in the alloy. Furthermore, smaller grain boundaries hinder the movement of dislocations, resulting in enhanced resistance to deformation and elevated microhardness values of the alloy.

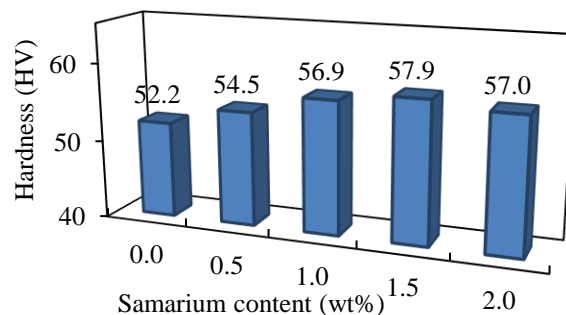


Figure 9 Effect of Sm addition on the hardness of ZRE1 alloy

4. Conclusions

The Addition of Sm led to the formation of a new phase of MgZn(CeSm) where Ce and Sm combined to form a secondary intermetallic phase surrounding the primary α -Mg grain. The formation of the intermetallic phase plays a major role in the improvement of the mechanical properties of the alloy. While the identification of these phases helped understand the strengthening mechanism of alloying treatment, Sm addition is effective for the UTS and YS improvement. The addition of Sm leads to intensive solution strengthening and increased dispersion strengthening of the secondary phase, thus resulting in mechanical strength improvement. The study shows that there is a strong relation between the microstructure and mechanical properties of the Sm-treated ZRE1 alloy. Coarser average grain size results in lower values of UTS, YS, elongation, and hardness. While finer average grain size produces alloys with better UTS, YS, elongation, and hardness. This is due to the secondary intermetallic phase containing RE, which can deter the dislocation movement, therefore improving the mechanical properties.

Acknowledgments

This research was supported by Universiti Tun Hussein Onn Malaysia (UTHM) through Research Enhancement-Graduate Grant (RE-GG) (vot Q203). Communication of this research is made possible through monetary assistance by UTHM Publisher's Office via Publication Fund E15216. Additional support in terms of facilities was also provided by Sustainable Manufacturing and Recycling Technology, Advanced Manufacturing and Material Center (SMART-AMMC), Universiti Tun Hussein Onn Malaysia (UTHM).

References

- Adrian, M., 2012. Titanium Alloys for Aerospace Structures and Engines A2. *Introduction to Aerospace Materials, Woodhead Publishing*, pp. 202–223
- Ahmad, R., Elaswad, A.M.M., Asmael, M.B.A., Shahizan, N.R., 2017a. Effect of Yttrium Addition on Microstructure and Hardness of Cast EV31A Magnesium Alloy. *Key Engineering Materials*, Volume 740, pp. 81–85
- Ahmad, R., Hamzah, M.Z., Asmael, M.B.A., Sheggaf, Z.M., 2016. Effects of Gadolinium on Microstructure and Hardness of Mg-Zn-Ce-Zr cast alloy. *ARPN Journal of Engineering and Applied Sciences*, Volume 11(14), pp. 8592–8597
- Ahmad, R., Sheggaf, Z.M., Asmael, M.B.A., Hamzah, M.Z., 2017b. Effect of Rare Earth Addition on Solidification Characteristics and Microstructure of ZRE1 Magnesium Cast Alloy. *Advances in Materials and Processing Technologies*, Volume 3(3), pp. 418–427
- Al-Alimi, S., Lajis, M.A., Shamsudin, S., 2017. Solid-State Recycling of Light Metal Reinforced Inclusions by Equal Channel Angular Pressing: A Review. *In: MATEC Web of Conferences*, Volume 135, p. 00013
- Al-Alimi, S., Lajis, M.A., Shamsudin, S., Yusuf, N.K., Chan, B.L., Didane, D.H., Rady, M.H., Sabbar, H.M., Msebawi, M.S., 2021. Development of Hot Equal Channel Angular Processing (ECAP) Consolidation Technique in the Production of Boron Carbide(B4C)-Reinforced Aluminium Chip (AA6061)-Based Composite. *International Journal of Renewable Energy Development*, Volume 10(3), pp. 607–621
- American Society for Testing and Materials (ASTM)., 2011. Standard Guide for Preparation of Metallographic Specimens. *In: American Society for Testing and Materials (ASTM) Book of Standards*

- Anawati, A., Asoh, H., Ono, S., 2018. Degradation Behavior of Coatings Formed by the Plasma Electrolytic Oxidation Technique on AZ61 Magnesium Alloys Containing 0, 1 and 2 wt% Ca. *International Journal of Technology*, Volume 9(3), pp. 622–630
- American Society for Testing and Materials (ASTM) International., 2015. Tension Testing Wrought and Cast Aluminum- and Magnesium-Alloy Products (Metric). In: *American Society for Testing and Materials (ASTM) Book of Standards*
- Chauhan, A., Lohra, S., Langyan, R., 2020. Synthesis and characterization of three ternary samarium(III) complexes and their optical properties. *Spectroscopy Letters*, Volume 53, pp. 595–606
- Chen, X., Li, Q., Chen, J., Zhu, L., 2019. Microstructure and Mechanical Properties of Mg- Gd-Y-Sm-Al Alloy and Analysis of Grain Refinement and Strengthening Mechanism. *Journal of Rare Earths*, Volume 37(12), pp. 1351–1358
- Chen, Y., Jin, L., Fang, D., Song, Y., Ye, R., 2015. Effects of Calcium, Samarium Addition on Microstructure and Mechanical Properties of AZ61 Magnesium Alloy. *Journal of Rare Earths*, Volume 33(1), pp. 86–92
- Ding-qian, D., 2008. Effect of Rare-earth La on Microstructure of Mg-4.5%Zn as-cast Magnesium Alloy. *Light Alloy Fabrication Technology*, Volume 36(10), pp. 11–13
- Enghag, P., 2004. Encyclopedia of the Elements: Technical Data, History, Processing, Applications. In: *Wiley-VCH*
- Ferro, R., Saccone, A., Delfino, S., 2013. Magnesium Alloys of the Rare Earth Metals: Systematics and Properties. *Metallurgical Science and Tecnology*, Volume 16(1)
- Geels, K., Fowler, D.B., Kopp, W.U., Rückert, M., 2007. Metallographic and Materialographic Specimen Preparation, Light Microscopy, Image Analysis and Hardness Testing. In: *West Conshohocken: ASTM international*
- Guan, K., Li, B., Yang, Q., Qiu, X., Tian, Z., Zhang, D., Zhang, D., Niu, X., Sun, W., Liu, X., Meng, J., 2018. Effects of 1.5 wt% samarium (Sm) addition on microstructures and tensile properties of a Mg–6.0Zn–0.5Zr alloy. *Journal of Alloys and Compounds*, Volume 735, pp. 1737–1749
- Hashmi, J.Z., Siraj, K., Latif, A., Naseem, S., Murray, M., Jose, G., 2019. The Role of Samarium Incorporated Structural Defects in ZnO Thin Films Prepared by Femtosecond Pulsed Laser Deposition. *Journal of Alloys and Compounds*, Volume 800, pp. 191–197
- Huang, Z.H., Liang, S.M., Chen, R.S., Han, E.H., 2009. Solidification Pathways and Constituent Phases of Mg-Zn-Y-Zr Alloys. *Journal of Alloys and Compounds*, Volume 468(1–2), pp. 170–178
- Institute of Rare Earths and Strategic Metals eV, 2020. Rare Earth Prices | Institute of Rare Earths and Strategic Metals eV. Available Online at <https://en.institut-seltenerden.de/our-service-2/Metal-prices/rare-earth-prices/>, Accessed on January 14, 2020
- Jahedi, M., McWilliams, B.A., Knezevic, M., 2018. Deformation and Fracture Mechanisms in WE43 Magnesium-rare Earth Alloy Fabricated by Direct-chill Casting and Rolling. *Materials Science and Engineering A*, Volume 726(March), pp. 194–207
- Júnior, P.F., De Olivé Ferreira, L., Garçaõ, W.J.L., De Paula Almeida, R., Melo, C.M., Ferreira, A.F., 2022. Heat-Flow Parameters Affecting Microstructure and Mechanical Properties of Al-Cu and Al-Ni Alloys in Directional Solidification: An Experimental Comparative Study. *International Journal of Materials Research*, Volume 113(3), pp. 181–193
- Ke-jie, L., Quan-an, L., Xiao-tian, J., Jun, C., Xing-yuan, Z., Qing, Z., 2009. Effects of Sm Addition on Microstructure and Mechanical Properties of Mg-6Al-0.6Zn Alloy. *Scripta Materialia*, Volume 60(12), pp. 1101–1104

- Kiani, M., Gandikota, I., Rais-rohani, M., Motoyama, K., 2017. Design of Lightweight Magnesium Car Body Structure Under Crash and Vibration Constraints. *Journal of Magnesium and Alloys*, Volume 2(2), pp. 99–108
- Kirman, Zulfia, A., Suharno, B., 2016. Effects of Magnesium on Properties of AlZrCe-Mg-Al₂O₃ Nanocomposites. *International Journal of Technology*, Volume 7(3), pp. 447–455
- Kristanto, G.A., Gusniani, I., Ratna, A., 2015. The performance of municipal solid waste recycling program in Depok, Indonesia. *International Journal of Technology*, Volume 6(2), pp. 264–272
- Kusrini, E., Ayuningtyas, K., Mawarni, D.P., Wilson, L.D., Sufyan, M., Rahman, A., Prasetyanto, Y.E.A., Usman, A., 2021. Micro-structured Materials for the Removal of Heavy Metals using a Natural Polymer Composite. *International Journal of Technology*, Volume 12(2), pp. 275–286
- Li, Q., Wang, Q., Wang, Y., Zeng, X., Ding, W., 2007. Effect of Nd and Y Addition on Microstructure and Mechanical Properties of as-cast Mg-Zn-Zr alloy. *Journal of Alloys and Compounds*, Volume 427(1–2), pp. 115–123
- Li, K., Xu, H., Tong, Z., 2019. Effects of Sm on Microstructure of Mg-12Gd-2Y-0.5Zr Alloy. In: IOP Conference Series: Materials Science and Engineering, Volume 569(2), p. 022017
- Liu, L., Chen, X., Pan, F., Gao, S., Zhao, C., 2016. A New High-strength Mg-Zn-Ce-Y-Zr Magnesium Alloy. *Journal of Alloys and Compounds*, Volume 688, pp. 537–541
- Liu, B.S., Wang, H.H., Zhang, Y.Z., Yang, Y.X., Ren, X.X., Du, H.Y., Hou, L.F., Wei, Y.H., Song, G.L., 2021. The influence of Adding Samarium on the Microstructure, Mechanical Performance and Corrosion Behavior of as-extruded AZ41 Alloys. *Journal of Physics and Chemistry of Solids*, Volume 150, p. 109851.
- Lucas, J., Lucas, P., Le-Mercier, T., Rollat, A., Davenport, W., 2014. Rare Earths Rare Earths Production and Use. In: *Elsevier B.V.*
- Luo, Q.Y., Luo, H., Kuang, H.M., Chen, W.T., Wen, Y.X., 2019. A novel samarium material: Synthesis, structure, photophysical properties and photoluminescence energy transfer mechanism. *Journal of Solid State Chemistry*, Volume 270, pp. 200–204
- Marzouk, S.Y., Hammad, A.H., 2020. Influence of Samarium Ions on the Structural, and Optical Properties of Unconventional Bismuth Glass Analyzed using the Judd–Ofelt Theory. *Journal of Luminescence*, Volume 231, p. 117772
- Materialstechnology, 2019. Weblinks : Magnesium Applications. TMS. Available Online at: www.materialstechnology.org, Accessed on March 03, 2021
- Moosbrugger, C., 2017. Engineering Properties of Magnesium Alloys. In: *ASM International (Issue M)*
- Pereira, P.H.R., Huang, Y., Langdon, T.G., 2017. Thermal Stability and Superplastic Behaviour of an Al-Mg-Sc alloy processed by ECAP and HPT at different temperatures. *IOP Conference Series: Materials Science and Engineering*, 194(1). <https://doi.org/10.1088/1757-899X/194/1/012013>
- Purnama, D., Winarto, W., Sofyan, N., Prihastomo, A., Ito, K., 2020. Microstructure and Mechanical Properties of Ah-36 Steel Weldment Welded using Magnesium Modified E6013 Electrode. *International Journal of Technology*. Volume 11(1), pp. 48–59
- Rady, M.H., Mahdi, A.S., Mustapa, M.S., Shamsudin, S., Lajis, M.A., Msebawi, M.S., Siswanto, W.A., Al Alimi, S., 2019. Effect of Heat Treatment on Tensile Strength of Direct Recycled Aluminium Alloy (AA6061). *Materials Science Forum*, Volume 961, pp. 80–87
- Rogal, L., Kania, A., Berent, K., Janus, K., Lityńska-Dobrzyńska, L., 2019. Microstructure and Mechanical Properties of Mg-Zn-RE-Zr Alloy After Thixoforming. *Journal of Materials Research and Technology*, Volume 8(1), pp. 1121–1131

- Rokhlin, L.L., Dobatkina, T.V., Tarytina, I.E., Luk'yanova, E.A., Temralieva, D.R., 2021. Effect of Samarium on the Recovery in Gadolinium-Containing Magnesium Alloys. *Russian Metallurgy (Metally)*, Volume 2021(7), pp. 816–820
- Ryou, H., Drazin, J.W., Wahl, K.J., Qadri, S.B., Gorzkowski, E.P., Feigelson, B.N., Wollmershauser, J.A., 2018. Below the Hall–petch Limit In Nanocrystalline Ceramics. *American Chemical Society (ACS) Nano*, Volume 4(12), pp. 3083–3094
- Rzychoń, T., Kielbus, A., Szala, J., 2008. Quantitative Description of Microstructure of ZRE1 Magnesium Alloy. *Inżynieria Materiałowa*, Volume 29(May), pp. 299–303
- Sadeq, M.S., Morshidy, H., 2020. Effect of Samarium Oxide on Structural, Optical and Electrical Properties of Some Alumino-borate Glasses with Constant Copper Chloride. *Journal of Rare Earths*, Volume 38, pp. 770–775
- Sheggaf, Z.M., Ahmad, R., Asmael, M.B.A., Elasad, A.M.M., 2017. Solidification, microstructure, and mechanical properties of the as-cast ZRE1 magnesium alloy with different praseodymium contents. *International Journal of Minerals, Metallurgy and Materials*, Volume 24, pp. 1306–1320
- StJohn, D.H., Qian, M., Easton, M.A., Cao, P., Hildebrand, Z., 2005. Grain refinement of magnesium alloys. *Metallurgical and Materials Transactions A*, Volume 36(7), 1669–1679
- Tekumalla, S., Seetharaman, S., Almajid, A., Gupta, M., 2014. Mechanical Properties of Magnesium-rare Earth Alloy Systems: A Review. *Metals*, Volume 5(1), pp. 1–39
- Wang, M.F., Xiao, D.H., Zhou, P.F., Liu, W.S., Ma, Y.Z., Sun, B.R., 2018. Effects of rare earth yttrium on microstructure and properties of Mg–Al–Zn alloy. *Journal of Alloys and Compounds*, Volume 742, pp. 232–239
- Wang, Y., Wu, G., Liu, W., Pang, S., Zhang, Y., Ding, W., 2014. Effects of Chemical Composition on the Microstructure and Mechanical Properties of Gravity Cast Mg-xZn- yRE-Zr alloy. *Materials Science and Engineering A*, Volume 594, pp. 52–61
- Yang, Z., Li, J.P., Zhang, J.X., Lorimer, G.W., Robson, J., 2008. Review on Research and Development of Magnesium Alloys. *Acta Metallurgica Sinica*, Volume 21(5), pp. 313–328
- Yunwei, G., Quanan, L., Xiaoya, C., Zhitao, L., 2018. As-cast Microstructures and Mechanical Properties of Mg-5Y-2Nd-xSm-0.5Zr (x = 0, 1, 3, 5). *Magnesium Alloys*, Volume 7(2), p. 58
- Zhang, Q., Wang, Y., Li, P., 2019. Grain-refinement Strengthening Effect of Y and Sm on Magnesium Alloy AZ81. *In: IOP Conference Series: Materials Science and Engineering*, Volume 592(1), p. 012027
- Zhang, Y., Huang, X., Li, Y., Ma, Z., Ma, Y., Hao, Y., 2017. Effects of Samarium Addition on as-cast Microstructure, Grain Refinement and Mechanical Properties of Mg-6Zn- 0.4Zr Magnesium Alloy. *Journal of Rare Earths*, Volume 35(5), pp. 494–502